

CrossMark
click for updatesCite this: *Chem. Sci.*, 2016, 7, 4364

Visible-light-driven CO₂ reduction on a hybrid photocatalyst consisting of a Ru(II) binuclear complex and a Ag-loaded TaON in aqueous solutions†

Akinobu Nakada, Takuya Nakashima, Keita Sekizawa, Kazuhiko Maeda and Osamu Ishitani*

A hybrid photocatalyst consisting of a Ru(II) binuclear complex and a Ag-loaded TaON reduced CO₂ by visible light even in aqueous solution. The distribution of the reduction products was strongly affected by the pH of the reaction solution. HCOOH was selectively produced in neutral conditions, whereas the formation of HCOOH competed with H₂ evolution in acidic conditions. Detailed mechanistic studies revealed that the photocatalytic CO₂ reduction proceeded via 'Z-schematic' electron transfer with step-by-step photoexcitation of TaON and the photosensitizer unit in the Ru(II) binuclear complex. The maximum turnover number for HCOOH formation was 750 based on the Ru(II) binuclear complex under visible-light irradiation, and the optimum external quantum efficiency of the HCOOH formation was 0.48% using 400 nm monochromatic light with ethylenediaminetetraacetic acid disodium salt as a sacrificial reductant. Even in aqueous solution, the hybrid could also convert visible-light energy into chemical energy ($\Delta G^{\circ} = +83 \text{ kJ mol}^{-1}$) by the reduction of CO₂ to HCOOH with methanol oxidation.

Received 6th February 2016

Accepted 23rd March 2016

DOI: 10.1039/c6sc00586a

www.rsc.org/chemicalscience

Introduction

The development of photocatalytic systems for CO₂ reduction is an attractive research target in the field of conversion of solar energy into chemical energy, the so-called artificial photosynthesis. Artificial photosynthetic reactions have various potential functions; one of these is to use water as both an electron source and as a solvent because water is an abundant and low-cost material. Since both CO₂ and water are very stable compounds, these photocatalytic systems should have both strong reduction and oxidation power. Utilization of visible light is another important function for artificial photosynthesis because it covers *ca.* 50% of the solar energy, whereas the light in the UV region ($\lambda < 400 \text{ nm}$) is very minor (<6%). However, there are few visible-light-driven photocatalysts for CO₂ reduction which function well in water.

Multinuclear Ru(II) and/or Re(I) diimine (N[^]N) complexes with a redox photosensitizer (PS) and a catalyst (CAT) unit, the so-called supramolecular photocatalysts, have attractive abilities as photocatalysts for CO₂ reduction because of their high efficiencies and selectivities for reducing CO₂ to HCOOH and

CO not only in organic solution¹⁻⁹ but also in aqueous solution.^{10,11} Since proton reduction to H₂ is a more thermodynamically favorable reaction than CO₂ reduction, this specific selectivity is a superior property for constructing an artificial photosynthesis system with CO₂ reduction in aqueous solution. However, the photocatalytic systems constructed with only metal complexes generally require a strong reductant such as NADH model compounds^{2,5-9} and benzimidazoline derivatives^{1,3,4,11} because the excited metal complexes have relatively weak oxidizing power. To add the stronger photooxidizing power, the metal complex photocatalyst should be combined with another photocatalyst for the oxidation reaction.

Some powder semiconductor photocatalysts with much stronger oxidizing power have been reported, which can oxidize even water involving reduction of electron acceptors.¹² Metal oxynitrides are typical examples; they have sufficient positive valence band potential to oxidize weak reductants and relatively small band gaps to utilize visible light.¹³

Based on these investigations regarding the strong and weak points of different types of photocatalysts, we have developed novel hybrid photocatalytic systems where supramolecular photocatalysts connect with metal oxynitride photocatalysts to utilize both the outstanding features of high selectivity and efficiency for CO₂ photoreduction (supramolecular site) and strong photooxidizing power (semiconductor site). Visible-light irradiation to the hybrid photocatalysts consisting of a Ru(II)

Department of Chemistry, Graduate School of Science and Engineering, Tokyo Institute of Technology, 2-12-1-NE-1 O-okayama, Meguro-ku, Tokyo 152-8550, Japan. E-mail: ishitan@chem.titech.ac.jp

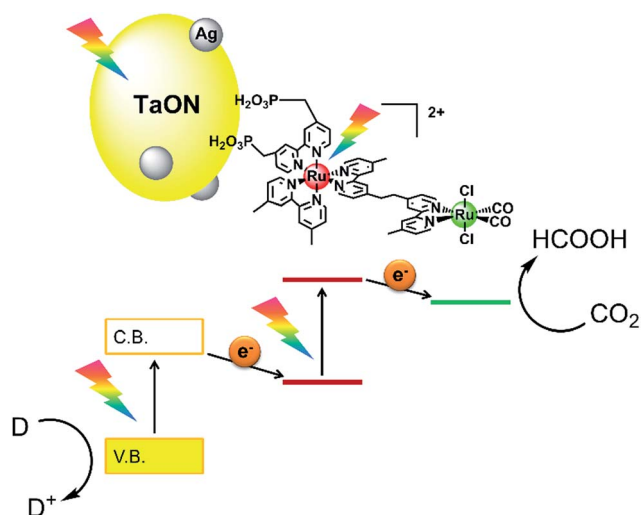
† Electronic supplementary information (ESI) available. See DOI: 10.1039/c6sc00586a



binuclear complex (**RuRu**) with $[\text{Ru}(\text{N}^{\wedge}\text{N})_3]^{2+}$ as the PS unit and $\text{Ru}(\text{N}^{\wedge}\text{N})(\text{CO})_2\text{Cl}_2$ as the CAT unit, which was adsorbed on a tantalum(v) oxynitride (TaON) photocatalyst in pure methanol without any other reductant under a CO_2 atmosphere, caused the catalytic formation of HCOOH as a reduced product of CO_2 and formaldehyde as an oxidized product of methanol (MeOH).¹⁴ Using CaTaO_2N instead of TaON in the hybrid achieved high selectivity of HCOOH formation (>99%) in dimethylacetamide–triethanolamine mixed solution; meanwhile, the photocatalytic reaction requires a sacrificial electron donor.¹⁵ These reactions are driven *via* the two-step photoinduced electron transfer mechanism, the so-called ‘Z-scheme’, as shown in Scheme 1: (1) step-by-step photoexcitation of the semiconductor and the Ru(II) PS unit occurs; (2) the valence band holes are consumed by a reductant; (3) conduction band electrons in the semiconductor transfer to the excited state of the PS unit, producing one-electron-reduced species (OERS) of PS; (4) intramolecular electron transfer from the OERS of the PS unit to the ground state of the CAT unit occurs, producing the reduced CAT unit and (5) CO_2 reduction proceeds on the reduced CAT.

Along with the Z-scheme hybrid photocatalysts, another powder hybrid photocatalyst consisting of a mononuclear metal complex as the CAT and a semiconductor such as carbon nitride^{16–18} or nitrogen-doped Ta_2O_5 ^{19,20} working as a PS have been developed for use in CO_2 reduction.

However, these hybrid photocatalysts were investigated only in organic solutions; we do not have any information on their photocatalytic activity in water. In this work, the photocatalytic activity of the hybrid photocatalyst of Ag-modified TaON and the Ru(II) binuclear complex (**RuRu**/Ag/TaON, Scheme 1) was investigated for the first time in aqueous solutions containing electron donors, and we observed that **RuRu**/Ag/TaON photocatalyzed efficient CO_2 reduction with high durability. This Z-schematic hybrid photocatalyst could also drive an uphill reaction, *i.e.* CO_2 reduction with methanol as a reductant, in a water–methanol mixed solution.



Scheme 1 Hybrid powder photocatalyst of the Ru(II) binuclear complex adsorbed on Ag-modified TaON (**RuRu**/Ag/TaON).

Results and discussion

A hybrid photocatalyst of Ag-modified TaON and a Ru(II) binuclear complex **RuRu**/Ag/TaON was synthesized according to a reported method.¹⁴ Typically, the loaded amount of silver and **RuRu** were 1.5 wt% and $3 \mu\text{mol g}^{-1}$, respectively, except for the experiment corresponding to Fig. 5. The obtained materials were characterized by diffuse reflectance spectroscopy (DRS), X-ray diffraction (XRD), emission spectroscopy and Fourier-transform infrared (FT-IR) spectroscopy, as shown in Fig. 1 and S1–S3, ESI.† The XRD patterns of TaON, Ag/TaON and **RuRu**/Ag/TaON confirm that the crystal structure of TaON was not changed during the attachment procedures of silver and **RuRu** on TaON (Fig. S1a, ESI†). The typical diffraction peak at $2\theta = 38.1^\circ$ is attributed to metallic silver; this peak appears in the spectra of Ag/TaON and **RuRu**/Ag/TaON (Fig. S1b, ESI†). Fig. 1 shows DRS spectra of the hybrids **RuRu**/Ag/TaON, Ag/TaON and TaON along with **RuRu**/ Al_2O_3 , which is a model of **RuRu**. A broad absorption band was observed in the cases of Ag/TaON and **RuRu**/Ag/TaON, which is due to surface plasmon resonance of the metallic silver particles on the surface of TaON. **RuRu**/Ag/TaON also exhibited an absorption attributable to the Ru(II) photosensitizer unit (Fig. 1 and S4, ESI†). A dispersion of **RuRu**/Ag/TaON in water showed emission with $\lambda_{\text{em}} = 629 \text{ nm}$ by photoexcitation at $\lambda_{\text{ex}} = 444 \text{ nm}$, which is attributable to phosphorescence from the triplet metal-to-ligand charge transfer ($^3\text{MLCT}$) excited state of the Ru(II) PS unit as well as phosphorescence from **RuRu** dissolved in water (Fig. S2, ESI†). IR absorption bands corresponding to the CO stretching vibrations of the Ru(II) CAT unit were observed at 2061 and 1997 cm^{-1} in the FT-IR spectrum of **RuRu**/Ag/TaON (Fig. S3, ESI†). These spectroscopic results indicate that the structure of **RuRu** was maintained after adsorption on Ag/TaON.

As a typical run, a powder of **RuRu**/Ag/TaON (4 mg) was dispersed in aqueous solution (4 mL) containing ethylenediaminetetraacetic acid disodium salt ($\text{EDTA} \cdot 2\text{Na}$, 10 mM) and irradiated at $\lambda_{\text{ex}} > 400 \text{ nm}$ under a CO_2 atmosphere. After 24 h irradiation, formic acid, H_2 and a small amount of CO were produced with turnover numbers (TON) of 750 ($8.5 \mu\text{mol}$), 1240



Fig. 1 DRS of **RuRu**/Ag/TaON (red), Ag/TaON (blue), TaON (green) and **RuRu**/ Al_2O_3 (black).



(14.2 μmol) and 30 (0.3 μmol), respectively (Fig. 2a). The external quantum yields (Φ) of the photocatalytic reaction were $\Phi_{\text{HCOOH}} = 0.47\%$ and $\Phi_{\text{H}_2} = 0.54\%$ using 400 nm monochromatic light. In contrast, formic acid was produced with much higher selectivity (85%) by addition of Na_2CO_3 (0.1 M) to the reaction solution (Fig. 2b), although $\text{TON}_{\text{HCOOH}}$ (620) and Φ_{HCOOH} (0.23%) were lower than those in the absence of Na_2CO_3 . Details of this difference are described in a later part of this paper.

The carbon source of HCOOH was confirmed by an isotope-labeling experiment. A red line in Fig. 3 shows the ^1H NMR spectrum of the reaction solution after the photocatalytic reaction under the same condition as that described above, except using $^{13}\text{CO}_2$ instead of ordinary CO_2 . A doublet attributed to H^{13}COOH was mainly observed at 8.31 ppm ($J_{\text{CH}} = 196$ Hz), with a small singlet attributed to H^{12}COOH . In contrast, only a singlet of H^{12}COOH was observed for the photocatalysis under ordinary CO_2 atmosphere (a blue line in Fig. 3). Based on the areas of these peaks, we calculated that 97% of HCOOH was formed by reduction of CO_2 in the photocatalytic reaction. Notably, this value is comparable with the purity of the $^{13}\text{CO}_2$ used (99%).

Table 1 summarizes the results of the photocatalytic reactions using various hybrids in aqueous solution containing $\text{EDTA}\cdot 2\text{Na}$ (10 mM). Irradiation to $\text{RuRu}/\text{Ag}/\text{Al}_2\text{O}_3$, where Al_2O_3 was used as an insulator instead of TaON, did not yield any reduction products (entry 2, Table 1). The oxidizing power of the excited photosensitizer unit in RuRu was evaluated by emission measurements using $\text{EDTA}\cdot 2\text{Na}$ as a quencher (Fig. S5, ESI †). Only 7% of the emission from the $^3\text{MLCT}$ excited state of the PS unit of RuRu on the surface of Al_2O_3 was quenched by 10 mM of $\text{EDTA}\cdot 2\text{Na}$. These results suggest that $\text{EDTA}\cdot 2\text{Na}$ mainly supplies electrons to the Ag/TaON unit in the photocatalytic reaction using $\text{RuRu}/\text{Ag}/\text{TaON}$. After the photocatalytic reaction using $\text{RuRu}/\text{Ag}/\text{TaON}$, we could not observe N_2 generation by gas chromatography. Furthermore, there were no differences in either the binding energy for the Ta4p peak or the ratio of areas for Ta4p and N1s of TaON in $\text{RuRu}/\text{Ag}/\text{TaON}$ before and after the photocatalytic reaction by X-ray photoelectron spectroscopy (XPS) analysis (Fig. S6, ESI †). These observations indicate that the TaON unit in $\text{RuRu}/\text{Ag}/\text{TaON}$ did not decompose during the photocatalytic reaction, which occasionally becomes a problem in some photocatalytic systems because it consumes



Fig. 3 ^1H NMR spectra of the aqueous reaction solutions (1 mL) containing $\text{RuRu}/\text{Ag}/\text{TaON}$ (4 mg) and $\text{EDTA}\cdot 2\text{Na}$ (10 mM), measured after 24 h irradiation at $\lambda_{\text{ex}} > 400$ nm under $^{13}\text{CO}_2$ (red) and $^{12}\text{CO}_2$ (blue) atmospheres.

photo-generated holes by the decomposition of TaON itself (eqn (1)).^{21–25}



Silver particles have been reported to act as a co-catalyst for CO_2 reduction on some semiconductor photocatalysts which require irradiation of UV light.^{26–34} However, Ag/TaON without RuRu did not photocatalyze CO_2 reduction at all (entry 3 in Table 1), indicating that the silver particles of $\text{RuRu}/\text{Ag}/\text{TaON}$ did not work as a co-catalyst for CO_2 reduction. However, loading silver to the surface of TaON dramatically enhanced the photocatalytic activity of $\text{RuRu}/\text{Ag}/\text{TaON}$, particularly for CO_2 reduction (compare entries 1 and 4, Table 1). It has been reported that loading of Ag on the surface of a hybrid photocatalyst $\text{RuRu}/\text{CaTaO}_2\text{N}$ enhances the photoinduced electron transfer from the conduction band of CaTaO_2N to the excited states of the Ru photosensitizer unit.¹⁵ A similar phenomenon

Table 1 Photocatalytic reactions using various hybrids under a CO_2 atmosphere^a

Entry	Photocatalyst	Product/ μmol (TON)		
		HCOOH	CO	H_2
1	$\text{RuRu}/\text{Ag}/\text{TaON}$	7.0 (600)	0.3 (28)	11.4 (978)
2	$\text{RuRu}/\text{Ag}/\text{Al}_2\text{O}_3$	N.D.	N.D.	N.D.
3	Ag/TaON	N.D.	N.D.	0.4 (—)
4	RuRu/TaON	1.2 (103)	0.2 (16)	5.0 (420)
5	$\text{Ru}(\text{Cat})^b/\text{Ag}/\text{TaON}$	<0.1 (—)	N.D.	<0.1 (—)
6	$\text{Ru}(\text{PS})^c/\text{Ag}/\text{TaON}$	<0.1 (—)	N.D.	4.2 (371)

^a Dispersion of a photocatalyst (4 mg) in an $\text{EDTA}\cdot 2\text{Na}$ (10 mM) aqueous solution (4 mL) was irradiated at $\lambda_{\text{ex}} > 400$ nm for 15 h. ^b $\text{Ru}(\text{Cat}) = \text{cis-Ru}\{4,4'-(\text{CH}_2\text{PO}_3\text{H}_2)_2-2,2'\text{-bipyridine}\}(\text{CO})_2\text{Cl}_2$. ^c $\text{Ru}(\text{PS}) = [\text{Ru}(\text{dmb})_2\{4,4'-(\text{CH}_2\text{PO}_3\text{H}_2)_2-2,2'\text{-bipyridine}\}](\text{PF}_6)_2$.

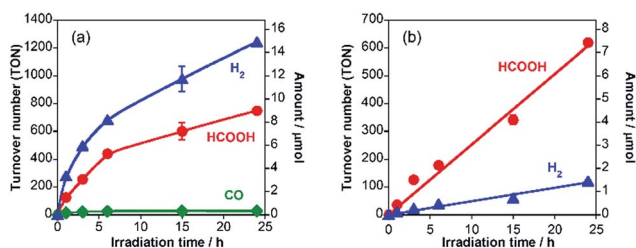


Fig. 2 Time courses of HCOOH (red), H_2 (blue) and CO (green) formation by visible-light ($\lambda > 400$ nm) irradiation to $\text{RuRu}/\text{Ag}/\text{TaON}$ (4 mg) in $\text{EDTA}\cdot 2\text{Na}$ (10 mM) aqueous solution (4 mL) without (a) and with (b) Na_2CO_3 (0.1 M) under a CO_2 atmosphere.



should accelerate the photocatalytic ability of **RuRu**/Ag/TaON in the present system.

Use of the mononuclear model complex of the CAT unit (**Ru(Cat)**) instead of **RuRu** drastically lowered the photocatalytic activity of the hybrid (entry 5, Table 1). This is reasonable because the electron transfer from the conduction band of TaON ($E_{\text{CBM}} = -1.31 \text{ V}$)¹⁴ to **Ru(Cat)** ($E_{\text{p}}^{\text{red}} = -1.46 \text{ V vs. Ag/AgCl}$ at pH 7)¹⁴ is an endergonic reaction. A hybrid without the catalyst unit (**Ru(PS)**/Ag/TaON), *i.e.* a mononuclear model complex of the PS unit (**Ru(PS)**) adsorbed on Ag/TaON, produced a catalytic amount of H₂ with a very small amount of HCOOH (entry 6, Table 1). There have been some reports that [Ru(N[^]N)₃]²⁺-type complexes decompose *via* photoinduced-ligand-substitution reactions to produce [Ru(N[^]N)₂(X)(Y)]ⁿ⁺-type complexes,^{35,36} and the product [Ru(N[^]N)₂(X)(Y)]ⁿ⁺ acts as a catalyst for both H₂ evolution and CO₂ reduction with the residual [Ru(N[^]N)₃]²⁺ as the photosensitizer.^{10,11,37} From these control experiments and the emission quenching measurements, we can conclude that all of the units in the hybrid photocatalyst **RuRu**/Ag/TaON are necessary for the efficient photocatalytic reduction of CO₂. **RuRu**/Ag/TaON worked *via* the Z-schematic electron-transfer mechanism from EDTA·2Na to the Ru catalyst unit with visible-light photoexcitation of both TaON and the Ru photosensitizer unit with the assistance of the Ag particles on the surface of TaON, followed by the CO₂ reduction proceeding on the Ru catalyst unit, as shown in Scheme 1.

The effects of coexistent ions and the pH of the reaction solution on the photocatalytic activity were examined in detail with a series of additional salts to the reaction solution. Table 2 summarizes the results using EDTA·2Na (10 mM) as an electron donor, including the produced amounts of the reduction products, the selectivity of CO₂ reduction (sel_{CO_2}) and the desorption ratios of the surface-bound **RuRu** (η_{des}). Addition of Na₂CO₃ (entry 2 in Table 2), K₂CO₃ (entry 3) and Na₂HPO₄ (entry 4), which changed the pH of the reaction solution to between

6.5 and 7.0, dramatically improved the selectivity of CO₂ reduction. On the other hand, the change in ion strength of the reaction solution should not be a reason for this change in selectivity because the selectivity did not change in reaction solutions containing various concentrations of NaH₂PO₄ (34–35%, pH = 4.4, entries 5–7), where the pH was similar to that without the salts (37%, pH = 4.3, entry 1). Fig. 4a (plots of entries 1–8 and 11) exhibit clear trend that higher pH increased the selectivity of CO₂ reduction unrelated to the ion strength of the solution; a more basic solution suppresses the evolution of H₂, probably because of the lower proton concentration in the reaction solution.

The produced amounts of HCOOH were lowered by the addition of the salts (0.1 M), regardless of the solution pH (entries 2–5). The UV-vis absorption spectra of the filtrates of the reaction solutions after the photocatalytic reactions exhibit an absorption band attributed to **RuRu** (Fig. S7, ESI[†]), indicating that **RuRu** partially desorbed from **RuRu**/Ag/Al₂O₃ during the photocatalytic reaction. Ru(II) diimine complexes with phosphonic acid anchor groups have been widely used as a photosensitizer in various photocatalytic systems^{14–19,38–41} and dye-sensitized photoelectrochemical cells.^{42–50} It was reported that in many cases, desorption of Ru complexes from the surface of metal oxides proceeded under visible-light irradiation in aqueous solution.^{51–54} The η_{des} s were 52–60% in the presence of the salts (0.1 M; entries 2–5), which were three times larger than those in the absence of the salts (entry 1). Higher concentration of salts in the reaction solution induced higher η_{des} and lower TON (Fig. 4b), while lower concentration of salts suppressed the desorption of the metal complex and deactivation of the photocatalytic reaction (entries 1 and 6–8 in Table 2 and Fig. 4b). On the other hand, the pH of the solution and the type of added salts did not strongly affect η_{des} (entries 2–5). A mixed system of Ag/TaON (4 mg) and a Ru(II) binuclear complex without the methyl phosphonate anchoring groups (12 nmol) showed much lower photocatalytic abilities (compare entry 1

Table 2 Results of photocatalytic reactions using **RuRu**/Ag/TaON (4 mg) in EDTA·2Na (10 mM) aqueous solutions containing various salts (4 mL) under visible-light ($\lambda > 400 \text{ nm}$) irradiation for 15 h

Entry	Salt ^a	pH ^b	Product/ μmol (TON)			sel_{CO_2} / ^c %	η_{des} / ^c %
			HCOOH	CO	H ₂		
1	None	4.3	7.0 (600)	0.3 (28)	11.4 (978)	37	17
2	Na ₂ CO ₃	7.0	4.0 (340)	N.D.	0.7 (60)	85	58
3	K ₂ CO ₃	7.0	3.7 (307)	N.D.	0.9 (74)	81	60
4	Na ₂ HPO ₄	6.5	5.6 (482)	<0.1	2.0 (172)	74	58
5	NaH ₂ PO ₄	4.4	3.2 (257)	<0.1	6.1 (481)	35	52
6	NaH ₂ PO ₄ ^d	4.4	3.9 (327)	<0.1	7.9 (658)	34	37
7	NaH ₂ PO ₄ ^e	4.4	4.8 (421)	0.2 (13)	9.0 (791)	34	32
8	Na ₂ HPO ₄ ^f + NaH ₂ PO ₄ ^f	6.1	4.8 (418)	<0.1	2.8 (245)	63	53
9 ^g	None	4.3	0.7 (56)	N.D.	0.5 (46)	32	—
10 ^h	None	4.3	1.3 (350)	<0.1	2.9 (773)	55	—
11 ⁱ	None	5.9	6.7 (589)	0.1 (12)	4.8 (418)	58	26

^a Concentration was 0.1 M except for entries 6–8. ^b After purging with CO₂ for 20 min. ^c Selectivity of CO₂ reduction. ^d Concentration was 0.03 M. ^e Concentration was 0.01 M. ^f Concentration was 0.05 M. ^g Using Ag/TaON (4 mg) and Ru(bpy)₂(CH₃bpyCH₂CH₂bpyCH₃)Ru(CO)₂Cl₂ (12 nmol). ^h Adsorption amount of **RuRu** was 1.0 $\mu\text{mol g}^{-1}$. ⁱ Using ethylenediaminetetraacetic acid tetrasodium salt (EDTA·4Na, 10 mM) instead of EDTA·2Na.



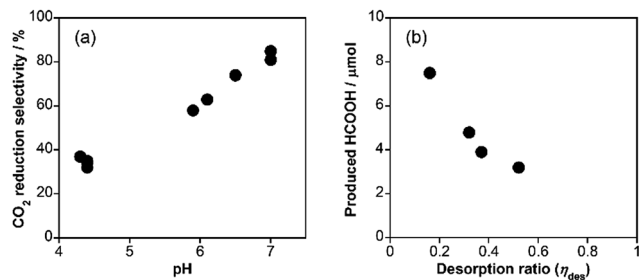


Fig. 4 (a) Selectivity of CO₂ reduction (sel_{CO₂}) vs. pH of the reaction solution in the photocatalytic reactions. (b) Produced amount of HCOOH vs. desorption ratio of RuRu (η_{des}) by the photocatalytic reactions with various concentration of NaH₂PO₄ (pH = 4.4).

and entry 9). Therefore, the addition of salts accelerated the desorption of RuRu, lowering the photocatalytic activity of RuRu/Ag/TaON. This is also supported by the following experimental data: the use of RuRu/Ag/TaON with a smaller amount of RuRu (1.0 μmol g⁻¹) produced much smaller amounts of HCOOH and H₂ (1.3 and 2.9 μmol, entry 10) compared with RuRu/Ag/TaON with 3.0 μmol g⁻¹ of RuRu (7.0 μmol of HCOOH and 11.4 μmol of H₂, entry 1). The details of the effects of the adsorbed amount of RuRu on the activity are described later. Taking into account these effects of pH and concentration of additives, higher selective HCOOH formation (58% selectivity) was obtained when ethylenediaminetetraacetic acid tetrasodium salt (EDTA·4Na, pH = 5.9; entry 11) was used instead of EDTA·2Na (pH = 4.3; entry 1) keeping high TON of 589 for HCOOH formation.

Fig. 5 shows the external quantum efficiencies for photocatalytic HCOOH production (Φ_{HCOOH}) using RuRu/Ag/TaON with various loading amounts of RuRu. The Φ_{HCOOH} increased with increasing loading amount of RuRu from 1.0 to 3.0 μmol g⁻¹ and then reached plateau with the maximum values of Φ_{HCOOH} = 0.48% at 8.3 μmol g⁻¹. This is probably why the separation of the electron-hole pairs in TaON was accelerated

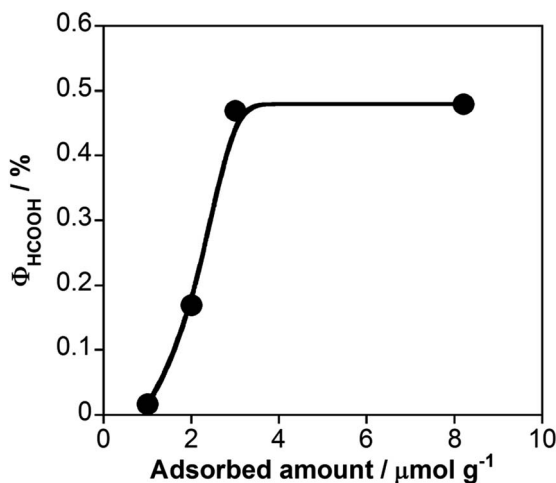


Fig. 5 Relationship between Φ_{HCOOH} and loading amount of RuRu in the photocatalytic reaction using RuRu/Ag/TaON (30 mg) and EDTA·2Na (10 mM) in aqueous solution (10 mL) with 400 nm monochromatic light irradiation under a CO₂ atmosphere.



Fig. 6 Time courses of HCOOH (red), H₂ (blue) and HCHO (green) formation along with the sum of HCOOH and H₂ (black broken line) in the photocatalytic reaction: RuRu/Ag/TaON (4 mg) in a H₂O–MeOH (4 : 1 v/v) mixed solution (4 mL) was irradiated by visible light (λ > 400 nm) under a CO₂ atmosphere. Inset shows enlarged time courses until 4 h irradiation.

because of the electron transfer from the conduction band to RuRu. The loading amount of 3.0 μmol g⁻¹ might be sufficient to produce this effect. Notably, Φ_{HCOOH} is the highest value obtained for photocatalytic CO₂ reduction using semiconductor–photosensitizer–catalyst triad systems to date.

We have already reported that RuRu/Ag/TaON can use methanol as a reductant for CO₂ reduction in pure methanol.¹⁴ This is important because CO₂ reduction with methanol oxidation producing HCOOH as a reduced product of CO₂ and HCHO as an oxidized product of methanol (eqn (2)) is an endergonic reaction (ΔG⁰ = +83 kJ mol⁻¹); in other words, the visible-light energy is converted into chemical energy *via* the photocatalytic CO₂ reduction reaction. As the next step, in this study, we investigated whether the same endergonic CO₂ conversion reaction can proceed even in aqueous solution. Fig. 6 shows a time course of the TONs of both reduction products (HCOOH and H₂) and an oxidation product (formaldehyde) in a photocatalytic reaction using RuRu/Ag/TaON in a H₂O–MeOH mixed solution (4 : 1 v/v) without any other reductants. HCOOH and H₂ were produced continuously and TON_{HCOOH} reached 17 at 3 h of irradiation. Formaldehyde was also formed, whose produced amount corresponded to the total of HCOOH and H₂ (Fig. 6 inset). This indicates that the overall reaction of the CO₂ reduction can be represented in eqn (2).



However, further irradiation induced less production of formaldehyde than the sum of HCOOH and H₂ (Fig. 6). We employed a ¹³C₂ labelling experiment to clarify the carbon sources of HCOOH. Fig. 7a shows the ¹H NMR spectrum of the filtered reaction solution after irradiation for 48 h; a doublet signal with ¹J_{CH} = 204 Hz and a singlet at 8.21 ppm are attributed to the methine protons of H¹³COOH and H¹²COOH, respectively. From this spectrum, we estimated that the main



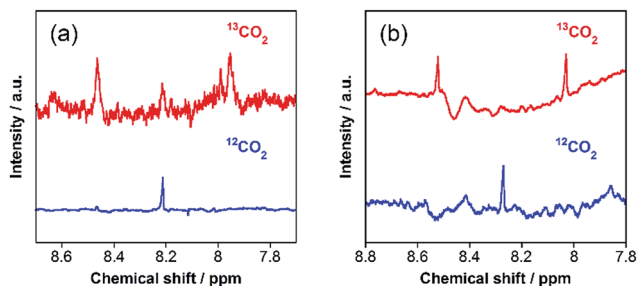


Fig. 7 ^1H NMR spectra of reaction solutions (2 mL) containing $\text{RuRu}/\text{Ag}/\text{TaON}$ (8 mg) in (a) H_2O - MeOH (4 : 1 v/v) and (b) H_2O - $i\text{PrOH}$ (4 : 1 v/v) after a 48 h irradiation with visible light ($\lambda > 400$ nm) under $^{13}\text{CO}_2$ (red) and $^{12}\text{CO}_2$ (blue) atmospheres.

carbon source of HCOOH was CO_2 (86%), although there were other carbon sources (14%). To gather information on the other carbon sources, a similar photocatalytic reaction was conducted using 2-propanol ($i\text{-PrOH}$) instead of methanol. This photocatalytic system also yielded HCOOH with $\text{TON}_{\text{HCOOH}} = 58$ after 15 h of irradiation but did not give any HCHO . Fig. 7b shows the result of a $^{13}\text{CO}_2$ labelling experiment using $i\text{-PrOH}$ as the reductant; the ^1H NMR spectrum of the filtered reaction solution after 48 h irradiation exhibits that the HCOOH was completely produced from CO_2 . Therefore, when methanol was used as the reductant, partial HCOOH produced in the photocatalytic reduction was probably generated by further oxidation of HCHO , which was produced by oxidation of the methanol. This is also supported by the following result: the photocatalytic oxidation of MeOH using TaON as a photocatalyst and AgNO_3 as a sacrificial oxidant in aqueous solution containing MeOH yielded not only HCHO as a main product but also HCOOH as a minor one (Fig. S8, ESI †). This minor formation process of HCOOH should contribute to determining the product distribution after a certain amount of HCHO was generated in the reaction solution. As described above, the ‘mismatch’ between the amount of HCHO and the total amount of HCOOH and H_2 was initially observed after a 6 h irradiation, and a longer irradiation increased this mismatch.

Experiments

General procedures

UV-vis absorption spectra were measured with a JASCO V-565 spectrophotometer. X-ray diffraction was measured with a Rigaku MiniFlex 600. FT-IR spectra were measured at 1 cm^{-1} resolution with a JASCO FT/IR-610 spectrophotometer. Emission spectra were measured at $298 \pm 0.1\text{ K}$ with a JASCO FP-6500 spectrofluorometer. Emission lifetimes were measured with a Horiba FluoroCube 1000U-S time-correlated single-photon-counting system (the excitation source was a nano-LED 440L, and the instrument response was less than 1 ns).

Materials

$\text{RuRu}/\text{Ag}/\text{TaON}$ was synthesized according to a literature procedure.¹⁴ Briefly, an AgNO_3 (137 μM) aqueous solution

(10 mL) was added dropwise to a dispersion (100 mg) of TaON in water (10 mL), followed by stirring for 2 h. Then the suspension was evaporated and the residue was heated at 473 K for 1 h under a H_2 atmosphere to obtain 1.5 wt% Ag -modified TaON (Ag/TaON). Then, a moderate amount of Ag/TaON was soaked in an acetonitrile solution of the $\text{Ru}(\text{II})$ binuclear complex (RuRu) for 3 h to obtain $\text{RuRu}/\text{Ag}/\text{TaON}$. The adsorption amount was estimated by the UV-vis absorbance changes of the solution before and after soaking (Fig. S4, ESI † shows an example of a RuRu adsorbed sample with a loading amount of $3\ \mu\text{mol g}^{-1}$).

$\text{Ag}/\text{Al}_2\text{O}_3$ and Ag/TiO_2 were prepared by the same impregnation-hydrogenation method followed by adsorption of RuRu as $\text{RuRu}/\text{Ag}/\text{TaON}$ for Al_2O_3 (AEROXIDE Alu C, AEROSIL) and TiO_2 (AEROXIDE TiO_2 P25, AEROSIL), respectively.

Tap water was purified using a Millipore Elix Essential 3 UV system and used on the same day. Methanol was used after distillation. Absolute 2-propanol was purchased from Kanto Chemical Co., Inc. and used without purification. Other materials were reagent-grade quality and were used without further purification.

Photocatalytic reactions

A suspension of photocatalyst (4 mg) in a reaction solution (4 mL) was prepared in an 8 mL test tube (i.d. = 8 mm) and purged with CO_2 . The suspensions were irradiated by stirring using a photocatalytic reactor (Koike Precision Instruments) at $\lambda > 400$ nm with a high-pressure Hg lamp combined with a NaNO_2 aqueous solution filter. The temperatures of the solutions were controlled at $298 \pm 2\text{ K}$ using an EYELA constant temperature system (CTP-1000) during irradiation. The quantum yield for HCOOH and H_2 formation was evaluated in a reaction cell containing $\text{RuRu}/\text{Ag}/\text{TaON}$ (30 mg) in a reaction solution (10 mL), which was irradiated with 400 nm monochromatic light using a 300 W Xe-lamp (Asahi Spectrum MAX-303) with a band pass filter (fwhm = 10 nm). The gaseous reaction products, *i.e.* CO and H_2 , were analyzed by a GC-TCD (GL Science GC 323). HCOOH in the liquid phase was analyzed by a capillary electrophoresis system (Otsuka Electronics Co. Capi-3300I). HCHO was quantitated by a colorimetric analysis following a reported procedure.¹⁴

We evaluated the photocatalytic activity of the hybrids by using turnover number (TON, eqn (3)), selectivity (eqn (4)) and external quantum efficiency (Φ , eqn (5)).

$$\text{TON} = \frac{\text{product}(\text{mol})}{\text{RuRu used}(\text{mol})} \quad (3)$$

$$\text{Selectivity} = \frac{\text{CO}_2 \text{ reduction product}(\text{mol})}{\text{reduction products}(\text{mol})} \quad (4)$$

$$\Phi = \frac{\text{product}(\text{mol})}{\text{imputed photon}(\text{einstein})} \quad (5)$$

$^{13}\text{CO}_2$ labelling experiments

$^{13}\text{CO}_2$ labelling experiments in $\text{EDTA}\cdot 2\text{Na}$ (10 mM) aqueous solution were performed using a dispersion of $\text{RuRu}/\text{Ag}/\text{TaON}$ (4 mg) in aqueous solution (1 mL) containing $\text{EDTA}\cdot 2\text{Na}$



(10 mM) in a reaction cell. The cell was degassed using the freeze–pump–thaw method, and then $^{13}\text{CO}_2$ (99%, 703 mmHg) was introduced into it. For the photocatalytic system in H_2O –MeOH mixed solution, a suspension of RuRu/Ag/TaON (8 mg) in a H_2O –MeOH (2 mL, 4 : 1 v/v) mixed solution in an 8 mL test tube was purged with $^{13}\text{CO}_2$ (99%) for 20 min. The suspensions were irradiated using a photocatalytic reactor (Koike Precision Instruments) at $\lambda > 400$ nm with a high-pressure Hg lamp combined with a NaNO_2 aqueous solution filter. After photolysis, the reaction solution was analyzed by ^1H NMR by using a JEOL ECA400II (400 MHz) system with a No-D technique following filtration.

Conclusions

A hybrid of a supramolecular photocatalyst with both Ru(II) photosensitizer and catalyst units, and Ag-loaded TaON photocatalyzed CO_2 reduction, even in aqueous solution; step-by-step photoexcitation of the Ru(II) photosensitizer unit and TaON could induce both strong reducing and oxidizing power in the hybrid photocatalyst, and relatively efficient CO_2 reduction giving HCOOH proceeded with high durability in aqueous solution containing EDTA·2Na as an electron donor. This Z-scheme-type hybrid photocatalyst could also induce reduction of CO_2 with methanol as the reductant giving HCOOH and HCHO even in aqueous solution, where the visible-light energy was converted into chemical energy ($\Delta G^0 = +83 \text{ kJ mol}^{-1}$).

Acknowledgements

This work was supported by CREST/JST and a Grant-in-Aid for Scientific Research on Innovative Areas “Artificial photosynthesis (AnApple)” (No. 24107005) from the Japan Society for the Promotion of Science (JSPS). K. M. acknowledges the Noguchi Institute for financial support. The authors also thank AEROSIL for supplying TiO_2 and Al_2O_3 materials.

References

- 1 Y. Tamaki, K. Koike and O. Ishitani, *Chem. Sci.*, 2015, **6**, 7213–7221.
- 2 E. Kato, H. Takeda, K. Koike, K. Ohkubo and O. Ishitani, *Chem. Sci.*, 2015, **6**, 3003–3012.
- 3 Y. Tamaki, K. Koike, T. Morimoto and O. Ishitani, *J. Catal.*, 2013, **304**, 22–28.
- 4 Y. Tamaki, K. Koike, T. Morimoto, Y. Yamazaki and O. Ishitani, *Inorg. Chem.*, 2013, **52**, 11902–11909.
- 5 Y. Tamaki, K. Watanabe, K. Koike, H. Inoue, T. Morimoto and O. Ishitani, *Faraday Discuss.*, 2012, **155**, 115–127.
- 6 Y. Tamaki, T. Morimoto, K. Koike and O. Ishitani, *Proc. Natl. Acad. Sci. U. S. A.*, 2012, **109**, 15673–15678.
- 7 K. Koike, S. Naito, S. Sato, Y. Tamaki and O. Ishitani, *J. Photochem. Photobiol., A*, 2009, **207**, 109–114.
- 8 S. Sato, K. Koike, H. Inoue and O. Ishitani, *Photochem. Photobiol. Sci.*, 2007, **6**, 454–461.
- 9 B. Gholamkhash, H. Mametsuka, K. Koike, T. Tanabe, M. Furue and O. Ishitani, *Inorg. Chem.*, 2005, **44**, 2326–2336.
- 10 A. Nakada, K. Koike, T. Nakashima, T. Morimoto and O. Ishitani, *Inorg. Chem.*, 2015, **54**, 1800–1807.
- 11 A. Nakada, K. Koike, K. Maeda and O. Ishitani, *Green Chem.*, 2016, **18**, 139–143.
- 12 A. Kudo and Y. Miseki, *Chem. Soc. Rev.*, 2009, **38**, 253–278.
- 13 K. Maeda, *Phys. Chem. Chem. Phys.*, 2013, **15**, 10537–10548.
- 14 K. Sekizawa, K. Maeda, K. Domen, K. Koike and O. Ishitani, *J. Am. Chem. Soc.*, 2013, **135**, 4596–4599.
- 15 F. Yoshitomi, K. Sekizawa, K. Maeda and O. Ishitani, *ACS Appl. Mater. Interfaces*, 2015, **7**, 13092–13097.
- 16 R. Kuriki, K. Sekizawa, O. Ishitani and K. Maeda, *Angew. Chem., Int. Ed.*, 2015, **54**, 2406–2409.
- 17 K. Maeda, R. Kuriki, M. Zhang, X. Wang and O. Ishitani, *J. Mater. Chem. A*, 2014, **2**, 15146–15151.
- 18 K. Maeda, K. Sekizawa and O. Ishitani, *Chem. Commun.*, 2013, **49**, 10127–10129.
- 19 T. M. Suzuki, H. Tanaka, T. Morikawa, M. Iwaki, S. Sato, S. Saeki, M. Inoue, T. Kajino and T. Motohiro, *Chem. Commun.*, 2011, **47**, 8673–8675.
- 20 S. Sato, T. Morikawa, S. Saeki, T. Kajino and T. Motohiro, *Angew. Chem., Int. Ed.*, 2010, **49**, 5101–5105.
- 21 G. Hitoki, T. Takata, J. N. Kondo, M. Hara, H. Kobayashi and K. Domen, *Chem. Commun.*, 2002, 1698–1699.
- 22 M. Hara, G. Hitoki, T. Takata, J. N. Kondo, H. Kobayashi and K. Domen, *Catal. Today*, 2003, **78**, 555–560.
- 23 M. Higashi, K. Domen and R. Abe, *Energy Environ. Sci.*, 2011, **4**, 4138–4147.
- 24 R. Abe, M. Higashi and K. Domen, *J. Am. Chem. Soc.*, 2010, **132**, 11828–11829.
- 25 K. Maeda, R. Abe and K. Domen, *J. Phys. Chem. C*, 2011, **115**, 3057–3064.
- 26 Z. Wang, K. Teramura, S. Hosokawa and T. Tanaka, *J. Mater. Chem. A*, 2015, **3**, 11313–11319.
- 27 K. Teramura, H. Tatsumi, Z. Wang, S. Hosokawa and T. Tanaka, *Bull. Chem. Soc. Jpn.*, 2015, **88**, 431–437.
- 28 Z. Wang, K. Teramura, S. Hosokawa and T. Tanaka, *Appl. Catal., B*, 2015, **163**, 241–247.
- 29 T. Takayama, K. Tanabe, K. Saito, A. Iwase and A. Kudo, *Phys. Chem. Chem. Phys.*, 2014, **16**, 24417–24422.
- 30 T. Takayama, A. Iwase and A. Kudo, *Bull. Chem. Soc. Jpn.*, 2015, **88**, 538–543.
- 31 K. Iizuka, T. Wato, Y. Miseki, K. Saito and A. Kudo, *J. Am. Chem. Soc.*, 2011, **133**, 20863–20868.
- 32 N. Yamamoto, T. Yoshida, S. Yagi, Z. Like, T. Mizutani, S. Ogawa, H. Nameki and H. Yoshida, *e-J. Surf. Sci. Nanotechnol.*, 2014, **12**, 263–268.
- 33 M. Yamamoto, T. Yoshida, N. Yamamoto, T. Nomoto, Y. Yamamoto, S. Yagi and H. Yoshida, *J. Mater. Chem. A*, 2015, **3**, 16810–16816.
- 34 M. Yamamoto, T. Yoshida, N. Yamamoto, T. Nomoto and S. Yagi, *Nucl. Instrum. Methods Phys. Res., Sect. B*, 2015, **359**, 64–68.
- 35 P. E. Hoggard and G. B. Porter, *J. Am. Chem. Soc.*, 1978, **100**, 1457–1463.
- 36 J. Van Houten and R. J. Watts, *Inorg. Chem.*, 1978, **17**, 3381–3385.



- 37 J.-M. Lehn and R. Ziessel, *J. Organomet. Chem.*, 1990, **382**, 157–173.
- 38 K. Maeda, M. Eguchi, S.-H. A. Lee, W. J. Youngblood, H. Hata and T. E. Mallouk, *J. Phys. Chem. C*, 2009, **113**, 7962–7969.
- 39 W. J. Youngblood, S.-H. A. Lee, K. Maeda and T. E. Mallouk, *Acc. Chem. Res.*, 2009, **42**, 1966–1973.
- 40 K. Maeda, G. Sahara, M. Eguchi and O. Ishitani, *ACS Catal.*, 2015, **5**, 1700–1707.
- 41 Y. Ueda, H. Takeda, T. Yui, K. Koike, Y. Goto, S. Inagaki and O. Ishitani, *ChemSusChem*, 2015, **8**, 439–442.
- 42 B. H. Farnum, A. Nakada, O. Ishitani and T. J. Meyer, *J. Phys. Chem. C*, 2015, **119**, 25180–25187.
- 43 G. Sahara, R. Abe, M. Higashi, T. Morikawa, K. Maeda, Y. Ueda and O. Ishitani, *Chem. Commun.*, 2015, **51**, 10722–10725.
- 44 B. D. Sherman, D. L. Ashford, A. M. Lapidés, M. V. Sheridan, K.-R. Wee and T. J. Meyer, *J. Phys. Chem. Lett.*, 2015, **6**, 3213–3217.
- 45 A. M. Lapidés, B. D. Sherman, M. K. Brennaman, C. J. Dares, K. R. Skinner, J. L. Templeton and T. J. Meyer, *Chem. Sci.*, 2015, **6**, 6398–6406.
- 46 M. V. Sheridan, B. D. Sherman, Z. Fang, K.-R. Wee, M. K. Coggins and T. J. Meyer, *ACS Catal.*, 2015, **5**, 4404–4409.
- 47 L. Alibabaei, B. D. Sherman, M. R. Norris, M. K. Brennaman and T. J. Meyer, *Proc. Natl. Acad. Sci. U. S. A.*, 2015, **112**, 5899–5902.
- 48 F. Li, K. Fan, L. Wang, Q. Daniel, L. Duan and L. Sun, *ACS Catal.*, 2015, **5**, 3786–3790.
- 49 X. Ding, Y. Gao, L. Zhang, Z. Yu, J. Liu and L. Sun, *ACS Catal.*, 2014, **4**, 2347–2350.
- 50 Y. Gao, X. Ding, J. Liu, L. Wang, Z. Lu, L. Li and L. Sun, *J. Am. Chem. Soc.*, 2013, **135**, 4219–4222.
- 51 K. Hanson, M. K. Brennaman, H. Luo, C. R. K. Glasson, J. J. Concepcion, W. Song and T. J. Meyer, *ACS Appl. Mater. Interfaces*, 2012, **4**, 1462–1469.
- 52 E. Bae, W. Choi, J. Park, H. S. Shin, S. B. Kim and J. S. Lee, *J. Phys. Chem. B*, 2004, **108**, 14093–14101.
- 53 K. Hanson, M. K. Brennaman, A. Ito, H. Luo, W. Song, K. A. Parker, R. Ghosh, M. R. Norris, C. R. K. Glasson, J. J. Concepcion, R. Lopez and T. J. Meyer, *J. Phys. Chem. C*, 2012, **116**, 14837–14847.
- 54 K. Hanson, M. D. Losego, B. Kalanyan, G. N. Parsons and T. J. Meyer, *Nano Lett.*, 2013, **13**, 4802–4809.

